

FUZZY INFERENCE SYSTEMS FOR STRUCTURAL DAMAGE ESTIMATION

Eleni VROCHIDOU¹, Petros-Fotios ALVANITOPOULOS², Ioannis ANDREADIS³,
Anaxagoras ELENAS⁴

ABSTRACT

This research provides a comparative study of intelligent systems in structural damage estimation after the occurrence of an earthquake. Structural safety and damage status of buildings after earthquakes is always in the forefront. Seismic response data of a reinforced concrete (RC) structure subjected to one-hundred different levels of seismic excitation are utilized to study the structural damage pattern. The structural damage is described by a well-known damage index, the Maximum Inter Story Drift Ratio (MISDR). Through a time-frequency analysis of the examined accelerograms, a set of seismic features is extracted. The relationship between seismic features and MISDR is investigated and proved to be strong. The aim of this paper is to analyze the performance of two different techniques for the set of the proposed seismic features; a Mamdani-type and a Sugeno-type fuzzy inference system (FIS). The performance of the models is evaluated in terms of the mean square error (MSE) between the actual calculated MISDR value and the estimated MISDR value derived from the proposed models, for the RC structure under the same seismic event. Experimental results show that the Mamdani FIS outperforms the Sugeno model in the case of MISDR estimation.

Keywords: Fuzzy inference system (FIS); Mamdani; Sugeno; Maximum inter-story drift ratio (MISDR); structural damage index

1. INTRODUCTION

This paper is motivated by the major problem of managing the damages and life-safe resources in urban areas after the manifestation of an earthquake. Its objective is to estimate potential structural damage on the affected area avoiding either nonlinear dynamic analysis of structures or post-seismic inspection of buildings. In order to perform structural damage estimation, two techniques based on FIS are developed. The fuzzy modeling techniques are based on Mamdani-type and Sugeno-type fuzzy models. The two models receive the same input data. The input data comprises an efficient set of newly extracted seismic intensity parameters. The results of the two FIS are compared. This paper underlines the differences between the two schemes and shows the better choice for the problem under study.

Among the data-driven methods, fuzzy methods are able to efficiently solve complex problems and reduce upcoming uncertainties. FIS are appealing for researchers and have found applications in various fields of science (Zhao et al. 2013; Song et al. 2013; Gao et al. 2012). The most appealing characteristic of fuzzy models is that they are able to describe complex and nonlinear problems (Zadeh

¹Dr., Department of Electrical and Computer Engineering, Democritus University of Thrace, GR-67100 Xanthi, Greece, evrochid@ee.duth.gr

²Dr., Department of Electrical and Computer Engineering, Democritus University of Thrace, GR-67100 Xanthi, Greece, palvanit@ee.duth.gr

³Professor, Department of Electrical and Computer Engineering, Democritus University of Thrace, GR-67100 Xanthi, Greece, indread@ee.duth.gr

⁴Professor, Department of Civil Engineering, Democritus University of Thrace, GR-67100 Xanthi, Greece, elenas@civil.duth.gr

1965). The fuzzy rules, which contain the input information, are easily interpretable. Furthermore, they provide a simple interface for extending the model with additional information by adding new rules or alternate the existing ones. The advantages of fuzzy techniques can be summarized as follows: 1) allow comprehensible definitions of knowledge of the system through "if-then" rules, 2) deal with the inherent uncertainties like experts approach their problems, 3) are based on a solid mathematical basis and 4) combine numerical and categorical data. Fuzzy techniques are reported in the literature for damage classification (Tsiftzis et al. 2006; Andreadis et al. 2007). The proposed fuzzy models are not restricted to classify the damage into damage categories but estimate numerically the structural damage degree. Classification results may be misleading since it is common to assign the damage that belongs to the edges of the predefined intervals in neighboring categories. However, by utilizing the proposed method, one can evaluate numerically the structural damage, providing the objective picture of the damage status.

The paper is organized as follows. Section 2 describes the seismic intensity features extraction process. Section 3 presents the motivation for the comparison of Mamdani versus Sugeno types of FIS and shows the development of the two schemes. Experimental results are illustrated in Section 4. Final conclusions are drawn in Section 5.

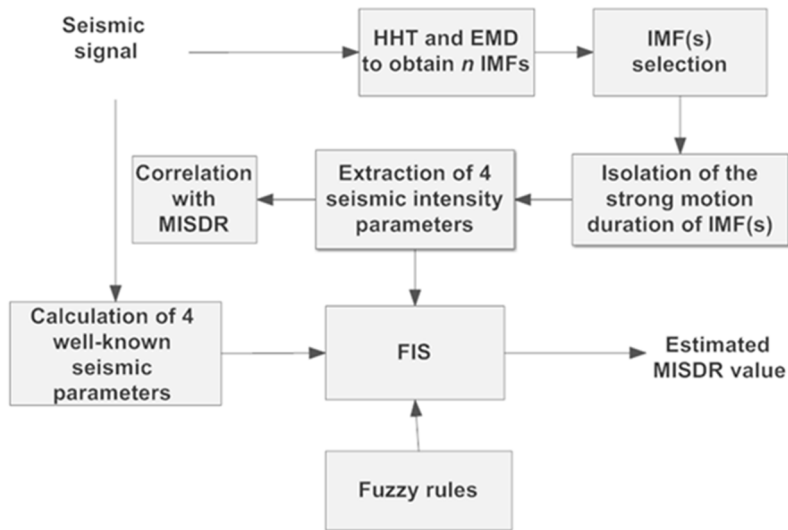


Figure 1. Proposed methodology

2. FUNDAMENTALS

This paper introduces two model schemes based on artificial intelligence techniques to relate inputs to outputs. The models receive the same set of input parameters that describe both the damage potential of seismic excitations and the characteristics of the structure under study. The structural damage degree is considered as the output of the models by means of a widely-used global damage index. More specifically, the fuzzy models receive as input a set of four well-known and four proposed seismic intensity parameters. These parameters are associated with the dissipated energy and the frequency content of the seismic accelerogram. The output of both models is a MISDR value which describes the seismic structural damage potential efficiently. Figure 1 demonstrates the proposed methodology. The seismic feature extraction process, the definition of the utilized structural damage index and details for the examined frame structure, are provided in the following subsections.

2.1 Seismic intensity features extraction

In this work, four well-known and four newly extracted seismic intensity parameters, calculated from the same original definitions, are utilized. Seismic intensity parameters are divided into four categories: spectral intensity, spectral, energy and peak parameters (Elenas and Meskouris 2001). One parameter from each category is selected and calculated for the entire seismic signal; the one that is

proven to be the most correlated to MISDR (Elenas and Meskouris 2001). These parameters are the Spectrum Intensity after Housner (SI_H), the spectral displacement (SD), the Arias Intensity (I_A) and the Peak Ground Velocity (PGV). The same set of parameters is also calculated for a specified subsection of the initial seismic signal to form the new modified set of seismic intensity parameters, referred as MSI_H , MSD, MI_A and MPGV. The proposed seismic intensity features extraction is according to a recent methodology (Vrochidou et al. 2016). The process is illustrated in Figure 1 and it is briefly reviewed below.

In the first step of the process, the Hilbert-Huang transform (HHT) (Huang et al. 1998) is performed. The HHT employs the ensemble empirical mode decomposition (EEMD) (Wu and Huang 2009) to decompose the signal into a finite number of intrinsic mode functions (IMFs). For each IMF is calculated the mean frequency value. When damage occurs to a structure, its eigenfrequency varies close to its original value. Thus, the IMF with mean frequency value closest (within a predetermined area) to the fundamental frequency of the examined structure is selected. Supposing that f_0 is the eigenfrequency of the structure, then the proposed area is between $0.9 f_0$ and $1.1 f_0$. The selected frequency band is based on the integration limits suggested by Kappos for the evaluation of spectrum intensity (Kappos 1990). If the closest mean frequency value belongs to this area, then the respective IMF is selected for further analysis. If the closest mean frequency value is spaced beyond the predetermined region then two IMFs, those that are located on either side of the region, are selected and summed.

In the second step of the process, an appropriate time-window of the selected IMF(s) is isolated. Two thresholds are specified for the time-window; t_{min} and t_{max} . t_{min} value is set to the time when the Husid diagram reaches the value 0.05, which is equal to the time when MISDR reaches the value 0.05, which is the 10% of the low-damage category threshold (set to 0.5) (Table 1). The t_{max} value is the time when the Husid diagram reaches the 80% of its maximum value, which is almost equal to the time when MISDR reaches 90% of its maximum value. The introduction of the time-window helps reduce the computational burden since, instead of the entire signal, only a part of one or two IMFs is imported to the following computer-supported analysis. Additionally, it represents a part of the earthquake duration where most of the seismic energy is released. Moreover, the time-window is directly related to the damage evolution of the examined structure. Finally, it helps eliminate the end effects issue (Huang 1998), one reported drawback of HHT, since the IMF edges are cut off. In this strong motion time-window are calculated the four aforementioned proposed seismic intensity parameters.

Table 1. Structural damage states according to MISDR.

Structural DI	Low	Medium	Large	Total
MISDR [%]	≤ 0.5	$0.5 < \text{MISDR} \leq 1.5$	$1.5 < \text{MISDR} \leq 2.5$	> 2.5

In the third step of the process, the set of 8 seismic parameters is input to the FIS, and the MISDR value is estimated for one hundred seismic events. The development of the FIS involves a tuning process, to optimize the number of membership functions. The tuning process is analyzed in Section 3.1.

2.2 Structural damage index MISDR

Damage indices summarize the damage evoked to a structure into a single value. MISDR can evaluate the level of the post-seismic damage of a structure and it is calculated according to the equation:

$$MISDR = \frac{|u|_{max}}{h} 100 [\%] \quad (1)$$

where $|u|_{max}$ is the maximum absolute inter-story drift and h the inter-story height (Structural Engineers Association of California 1995). The intervals of MISDR values are stated in Table 1. According to the ranges provided, the damage degree is classified in low, medium, large or total. These categories refer to minor, repairable, irreparable and severe damage or collapse of the building, respectively.

2.3 RC structure frame model

Figure 2 demonstrates the examined RC frame structure. The eigenfrequency of the 8-story model is 0.85 Hz. The frame is designed according to Eurocode rules EC2 (2000) and EC8 (2004). The cross-sections of the beams are T-beams with 40 cm width, 20 cm slab thickness, 60 cm total beam height and 1.45 m effective slab width. The distance between the frames of the structure is 6 m. The frame structure has been characterized as an "importance class II and ductility class medium" according to EC8. The subsoil is of type C and the region seismicity belongs to category 2. External loads are included and are corporate into load combinations as suggested in EC2 and EC8. After the design of the frame, a nonlinear dynamic analysis takes place and its structural seismic response (MISDR) is calculated through the computer program IDARC (Reinhorn et al. 2009).

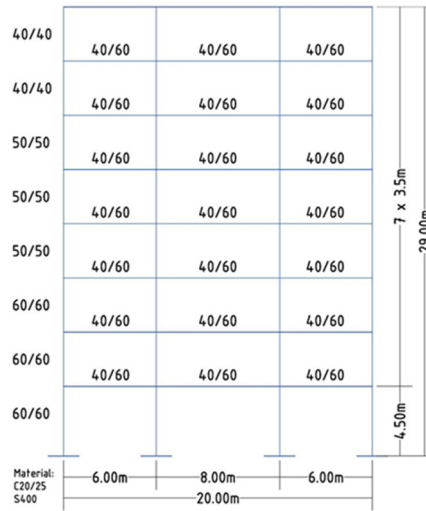


Figure 2. RC frame model

2.4 Correlation analysis

The examined fuzzy models predict a MISDR value based upon the inserted input data. In order to evaluate the efficiency of the seismic intensity parameters, which will be utilized subsequently as input data to the proposed fuzzy models, a correlation analysis is carried out. The relation between the seismic intensity parameters and the structural damage index MISDR is investigated. For this purpose, a correlation study based on Spearman rank correlation coefficient is carried out. For a set of n measurements of X and Y, where $i=1, 2, \dots, n$, the Spearman correlation coefficient is defined as:

$$P_{Spearman} = 1 - \frac{6 \sum_{i=1}^n D^2}{n(n^2 - 1)} \quad (2)$$

where D is the difference between the ranking degree of X and Y, respectively. Correlation coefficient values greater than 0.8, indicate a strong interrelation between the parameters. Less than 0.45 indicate weak connection and all other cases between 0.45 and 0.8 reveal medium connection (Elenas 2001). Correlation between MISDR and the selected seismic parameters are presented in Table 2. Strong interrelation with MISDR is revealed for the set of seismic parameters, greater than 0.81 in all cases.

Table 2. Rank correlation coefficients after Spearman.

	Seismic parameters							
	I _A	MI _A	SI _H	MSI _H	SD	MSD	PGV	MPGV
MISDR	0.85	0.87	0.92	0.81	0.89	0.85	0.82	0.82

3. MAMDANI VERSUS SUGENO FIS

FIS have two types based on the mathematical calculation of the inference: the Mamdani-type (Mamdani 1977) and the Sugeno-type inference (Sugeno 1977). A Mamdani-type fuzzy rule is described as follows: "If A is X1 and B is X2 then C is X3", where A, B, C are variables and X1, X2, X3 are fuzzy sets. A Sugeno-type fuzzy rule is described as follows: "If A is X1 and B is X2 then C= aA+bB+c", where a, b, c are constants, A, B, C are variables and X1, X2, X3 are fuzzy sets.

The main difference between the two schemes is in the evaluation of the output membership functions (MFs). In Sugeno-type FIS the output MF is a constant or linear function (allows a single output) while in Mamdani-type it is a fuzzy set (allows multiple outputs). Mamdani-type FIS uses defuzzification technique of the fuzzy output. Sugeno-type FIS uses a weighted average to compute a crisp output. Thus, Mamdani FIS provides an interpretable output. On the other hand, Sugeno FIS is more computationally efficient and has a better processing time as the weighted average technique replaces the time-consuming defuzzification procedure. Moreover, the Sugeno FIS is more flexible as it permits more than one parameters in the output. The output of Sugeno FIS is a function of the inputs; hence, it expresses a more distinct relation between them.

Here, the output of the model is a single numerical MISDR value. For problems of multiple inputs and one output, both models can be equally utilized and a performance comparison between them can be provided.

3.1 Development of the Mamdani FIS

MISDR damage estimation is initially developed by utilizing the Mamdani-type FIS model. The model receives 8 input parameters and provides one output; the MISDR estimated value. The rule-base is constructed from the input-output pairs. Input and output ranges are divided into fuzzy regions. Every region is determined by a MF. The performance of the model has been tested for successive values of MFs, starting from 4. The number of MFs has been increased until the best result has been obtained. The performance of the FIS is evaluated in terms of the MSE between the actual calculated MISDR value and the estimated MISDR value derived from the FIS, according to the equation:

$$MSE = \frac{1}{v} \sum_{j=1}^v |MISDR_{\text{calculated}} - MISDR_{\text{estimated}}|^2 \quad (3)$$

where v is the number of samples (the set of examined seismic events). Figure 3 demonstrates the evolution of the average MSE for different number of MFs. Optimal performance is achieved for 10 MFs for input and output parameters.

The parameters that define the MFs are subsequently defined through a genetic algorithm (GA) (Sivanandam and Deepa 2008). The determination of the appropriate parameters is an optimization problem. GAs are extensively employed to resolve fuzzy optimization problems (Kaya and Alhadj 2011; Tang et al. 1998). Triangular MFs are utilized in this work. In order to define a triangular MF is essential to designate three variables, the minimum, center and maximum values. These values are determined by the tuning process. For 8 input parameters and one output of 10 MFs each, the tuning variables rise to 270. An objective function is required to evaluate the potential solutions. The objective function of this work is the MSE between the calculated and the estimated value of MISDR defined from Equation 3. The GA searches for the optimal solution to minimize the MSE. It starts with

20 individuals as initial population. The optimized parameters are encoded in a vector of double values and scaling function is set to rank. A number of genetic operators are utilized. The selection function is roulette, crossover function is scattered, mutation technique is Gaussian and migration direction is forward. The number of generation is set to 100 and fitness tolerance to the order of 10^{-8} .

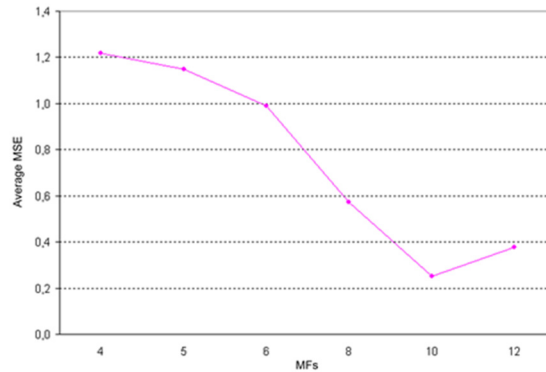


Figure 3. Average MSE for MISDR estimation according to the number of MFs

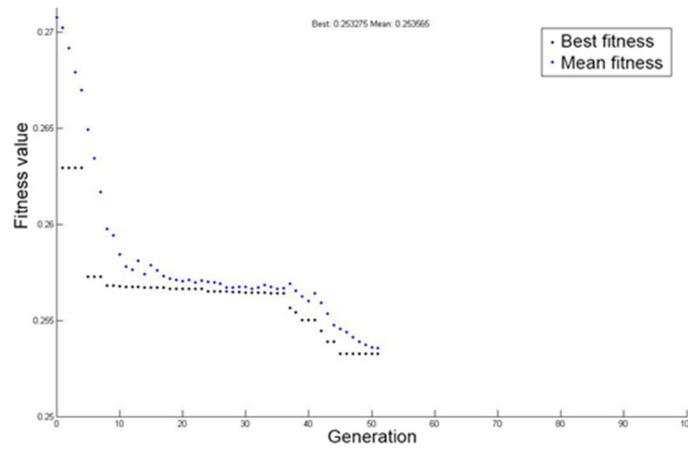


Figure 4. Evolution of objective value in the GA optimization

Figure 4 illustrates the evolution of the objective value during the optimization process. The GA finishes after 51 iterations due to fitness tolerance. Figure 5 demonstrates the MFs for the FIS input variables IA and MPG as determined by the optimization process.

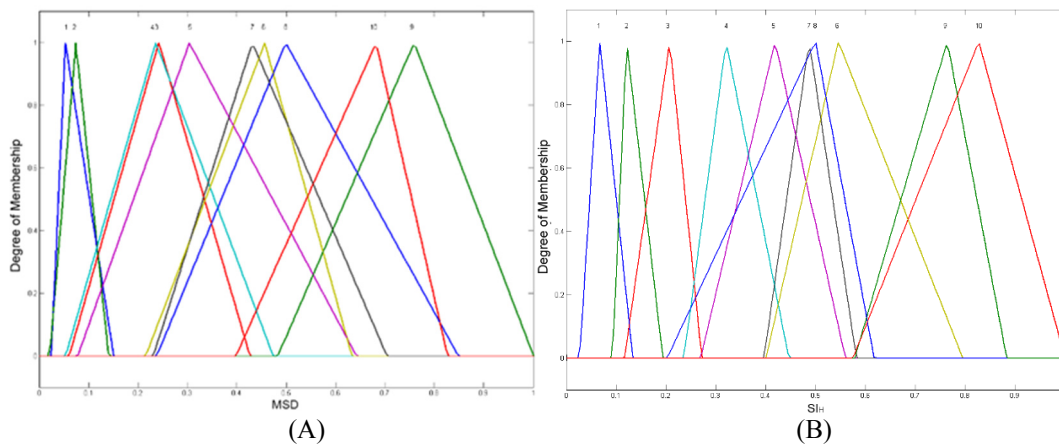


Figure 5. Ten tuned MFs for the FIS input variables (A) MSD and (B) SI_H

3.2 Development of the Sugeno FIS

The development of the MISDR damage estimation model utilizing Sugeno FIS is the same as the Mamdani FIS. In order the two models to be directly comparable, all initial setting remains the same. The model receives the same set of information from 8 input parameters and derives one output, the MISDR estimation value. The rule-base for the Sugeno FIS is the same as for the Mamdani FIS. Same remains the triangular MFs for the input parameters as there were defined from the optimization process.

Table 3. Examined ground motions (Natural earthquakes are marked in bold font).

No	Earthquake [Date/Station/Component]	MISDR Calculated	No	Earthquake [Date/Station/Component]	MISDR Calculated
1	Kobe [Jan16,1995/KJM/000]	7.88	51	Imperial Valley [Oct15,1979/E.C.C. FF/002]	1.48
2	Tabas(art.1) [Sep16,1978/Tabas/LN]	6.15	52	Erzican [Mar13,1992/Erzican/ EW]	1.40
3	Tabas [Sep16,1978/Tabas/TR]	5.95	53	Northridge [Jan17,1994/C.Coun./000]	1.35
4	Gazli(art.1) [Mai17,1976/Karakyr/000]	5.79	54	Erzican(art.3) [Mar13,1992/ Erzican/ EW]	1.29
5	Tabas [Sep16,1978/Tabas/LN]	5.16	55	Friuli [May 06,1976/ Conegliano/000]	1.17
6	Gazli(art.2) [May17,1976/Karakyr/000]	5.11	56	Coyote Lake[Aug 06,1979/C.Lk D-S.M./160]	1.04
7	Tabas(art.2) [Sep16,1978/Tabas/LN]	4.82	57	Round Valley [Nov23,1984/ M.C.S./270]	0.95
8	Tabas (art.1) [Sep16,1978/Tabas/TR]	4.66	58	Kocaelli [Aug17,1999/ Duzce/180]	0.943
9	Tabas(art.3) [Sep16,1978/Tabas/LN]	4.56	59	Baja(art.1) [Feb07,1987/Cerro Prieto/161]	0.94
10	Kobe(arti.1) [Jan16,1995/KJM/000]	4.49	60	Baja(art.2) [Feb07,1987/Cerro Prieto/161]	0.91
11	Gazli(art.3) [May17,1976/Karakyr/000]	4.28	61	Baja(art.3) [Feb07,1987/Cerro Prieto/161]	0.89
12	Tabas(art.1) [Sep16,1978/Dayhook/LN]	4.21	62	Baja [Feb07,1987/Cerro Prieto/161]	0.88
13	Kobe(art.2) [Jan16,1995/KJM/000]	3.88	63	Oroville [Aug02,1975/Med.Center/246]	0.87
14	Kobe(art.3) [Jan16,1995/KJM/000]	3.84	64	Oroville(art.1) [Aug02,1975/Med.Center/246]	0.8
15	Erzican(art.1) [Mar13,1992/Erzican/NS]	3.65	65	Oroville(art.2) [Aug02,1975/Med.Center/246]	0.79
16	Erzican [Mar13,1992/Erzican/NS]	3.63	66	Oroville(art.3) [Aug02,1975/Med.Center/246]	0.78
17	Tabas (art.2) [Sep16,1978/Tabas/TR]	3.51	67	Victoria(art.1) [Jun09,1980/Chihuahua/102]	0.71
18	Erzican(art.2) [Mar13,1992/Erzican/NS]	3.34	68	Chi-Chi [Sep 20, 1999/Chy025/E]	0.67
19	Tabas(art.3) [Sep16,1978/Tabas/TR]	3.31	69	Victoria(art.2) [Jun09,1980/Chihuahua/102]	0.66
20	Dinar [Jan10,1995/Dinar/090]	3.00	70	Victoria(art.3) [Jun09,1980/Chihuahua/102]	0.65
21	San Salvador [Oct10,1986/G.I.Cent./090]	2.95	71	Victoria [Jun09,1980/Chihuahua/102]	0.64
22	Dinar(art.1) [Jan10,1995/Dinar/090]	2.86	72	Coalinga [May02,1983/P.-C.C. Sc./360]	0.60
23	Northridge(art.1) [Jan17,1994/C.Coun./000]	2.74	73	Spitak(art.1) [Dec07,1988/Gukasian/000]	0.57
24	Northridge(art.2) [Jan17,1994/C.Coun./000]	2.68	74	Spitak [Dec07,1988/Gukasian/000]	0.552
25	Victoria [Jun 09, 1980/Cerro Prieto/045]	2.52	75	Spitak (art.2) [Dec07,1988/Gukasian/000]	0.54
26	San Salvador(art.1) [Oct10,1986/G.I.Cent./090]	2.45	76	Tabas [Sep16,1978/Dayhook/ LN]	0.45
27	Duzce [Nov12,1999/Bolu/000]	2.39	77	Coalinga [Jul22,1983/ CHP/000]	0.42
28	Duzce(art.1) [Nov12,1999/Bolu/000]	2.38	78	San Fernando [Feb09,1971/ Fort Tejon/000]	0.395
29	Kobe [Jan16,1995/Nishi-Akashi/000]	2.37	79	Hector Mine [Oct16,1999/Amboy/000]	0.39
30	San Salvador(art.2) [Oct10,1986/G.I.Cent./090]	2.36	80	Superstition Hills [Nov24,1987/KRN/270]	0.38
31	Victoria(art.1) [Jun09,1980/ Cerro Prieto/045]	2.31	81	Mt Lewis [Mar31,1986/Halls Valley/000]	0.37
32	Kobe(art.1) [Jan16,1995/ Nishi-Akashi/000]	2.23	82	Kocaelli [Aug17,1999/Eregli/090]	0.35
33	Duzce(art.1) [Nov12,1999/ Duzce/180]	2.17	83	Cape Mendocino [Apr25,1992/E.-M/000]	0.345
34	Duzce(art.2) [Nov12,1999/ Duzce/180]	2.13	84	Duzce [Nov12,1999/1058/E]	0.34
35	Duzce(art.2) [Nov12,1999/ Bolu/000]	2.09	85	Loma Prieta [Oct18,1989/C.L.D.D./195]	0.335
36	Cape Mendocino [Apr25,1992/Cape M. /000]	2.03	86	Parkfield [Jun28,1966/Cholame #8/050]	0.33
37	San Salvador(art.3) [Oct10,1986/G.I.Cent./090]	2.01	87	Loma Prieta (art.1) [Oct18,1989/UCSC/000]	0.30
38	Duzce(art.3) [Nov12,1999/Duzce/180]	1.99	88	Loma Prieta (art.2) [Oct18,1989/UCSC/000]	0.28
39	Duzce (art.3) [Nov12,1999/Bolu/000]	1.98	89	Coalinga Park [May02,1983/P.-F.Z16/090]	0.27
40	Victoria(art.2) [Jun09,1980/Cerro Prieto/045]	1.93	90	Loma Prieta [Oct18,1989/UCSC/000]	0.26
41	Dinar(art.2) [Jan10,1995/Dinar/090]	1.85	91	Loma Prieta (art.3) [Oct18,1989/UCSC/000]	0.25
42	Victoria(art.3) [Jun09,1980/Cerro Prieto/045]	1.81	92	West Moreland [Apr26,1981/B. Air./225]	0.245
43	Erzican(art.1) [Mar13,1992/Erzican/ EW]	1.79	93	Double Springs Eq [Sep12,1994/Wood./000]	0.24
44	Erzican(art.3) [Mar13,1992/Erzican/ NS]	1.69	94	Duzce Lam [Nov12,1999/L.st.531/N]	0.23
45	Dinar(art.3) [Jan10,1995/Dinar/090]	1.65	95	Hollister [Jan26,1920/H. D.Array #1/255]	0.18
46	Erzican(art.2) [Mar13, 1992/Erzican/ EW]	1.60	96	Calindar [Nov24,1976/St.Code:37/ S49E]	0.11
47	Superstition Hills(art.1)[Nov24,1987/KRN/270]	1.59	97	San Francisco(art.1) [Mar22,1957/1117/010]	0.10
48	Duzce [Nov12,1999/Duzce/180]	1.54	98	San Francisco [Mar22,1957/1117/010]	0.09
49	Gazli [May17,1976/Karakyr/000]	1.52	99	San Francisco(art.2) [Mar22,1957/1117/010]	0.08
50	Northridge(art.3) [Jan17,1994/C.Coun./000]	1.51	100	Irpinia Eq [Nov23,1980/Arienza/000]	0.07

4. EXPERIMENTAL RESULTS

A set of 100 seismic excitations, natural and artificially generated, are utilized to train and test the two models. Natural accelerograms are derived from the Pacific Earthquake Engineering Research Center

(PEER 2017). Artificial accelerograms are derived from the natural accelerograms, utilizing the methodology suggested by Vrochidou et al. (2014). The final data set of seismic excitations covers a wide range of MISDR values and displays a uniform formation; 25 accelerograms in each one of the 4 seismic categories according to the MISDR calculated values. Table 3 provides the necessary information (seismic event, country, date, station and component) for the set of 100 accelerograms. In Table 3 are also included the calculated MISDR values for the seismic events regarding the examined structure. The FIS models are trained with the eight selected seismic parameters of ninety-nine seismic signals.

One seismic signal is tested every time. Table 4 presents the MISDR estimation achieved with the Mamdani and Sugeno FIS, for every seismic event. The MSE between the estimated and the calculated value of MISDR for every seismic event with the two models is included in Table 5. The average MSE for all experiments is 0.253 with Mamdani-type FIS and 0.289 with Sugeno-type FIS. The results obtained show that for the given application of structural damage estimation, Mamdani-type FIS and Sugeno-type FIS work rather similarly.

Table 4. MISDR estimation values with Mamdani and Sugeno FIS (Misclassified signals are marked in bold font).

No. of event	MISDR estimation		No. of event	MISDR estimation		No. of event	MISDR estimation		No. of event	MISDR estimation	
	Mamdani	Sugeno		Mamdani	Sugeno		Mamdani	Sugeno		Mamdani	Sugeno
1	4.92	4.92	26	2.38	2.03	51	0.77	1.84	76	0.50	1.19
2	6.08	5.4	27	2.55	2.89	52	2.03	1.86	77	0.32	0.315
3	5.40	5.11	28	2.10	2.21	53	1.60	1.68	78	0.31	0.316
4	4.94	4.94	29	2.32	2.3	54	2.15	1.69	79	0.35	1.16
5	5.17	5.17	30	2.40	2.46	55	1.33	1.33	80	0.64	0.729
6	5.80	5.3	31	2.12	2.12	56	1.52	1.19	81	0.32	0.123
7	5.45	4.96	32	1.51	1.59	57	1.33	0.957	82	0.32	0.315
8	5.34	4.75	33	2.06	1.65	58	1.65	1.26	83	0.51	0.509
9	3.94	3.94	34	1.61	1.75	59	1.83	1.99	84	0.47	0.122
10	3.94	3.94	35	2.10	2.1	60	1.25	1.47	85	0.36	0.325
11	4.31	5.27	36	1.81	1.83	61	1.49	1.43	86	0.51	0.571
12	5.39	3.1	37	2.84	2.47	62	1.70	1.95	87	0.50	0.388
13	3.94	3.66	38	2.05	2.1	63	1.13	1.19	88	0.32	0.317
14	3.94	3.94	39	2.13	2.11	64	1.02	1.44	89	0.31	0.455
15	3.94	4.53	40	1.69	2.39	65	0.70	0.7	90	0.15	0.315
16	3.94	3.94	41	1.56	2.13	66	0.87	0.509	91	0.45	0.357
17	3.04	3.83	42	2.10	1.76	67	0.76	0.696	92	0.13	0.421
18	3.77	2.44	43	2.21	1.99	68	1.19	1.46	93	0.13	0.122
19	3.95	3.94	44	1.65	1.67	69	0.80	0.767	94	0.16	0.315
20	2.91	2.5	45	1.80	2.41	70	0.76	0.799	95	0.13	0.125
21	2.12	2.55	46	2.11	2.1	71	0.74	0.771	96	0.13	0.122
22	2.32	2.07	47	1.83	2.4	72	0.50	0.593	97	0.12	0.12
23	3.94	2.1	48	2.01	2.29	73	0.51	0.587	98	0.15	0.122
24	2.80	2.1	49	1.94	1.94	74	0.51	0.509	99	0.15	0.122
25	2.63	1.93	50	2.20	1.89	75	0.51	0.639	100	0.12	0.12
4th damage category			3rd damage category			2nd damage category			1st damage category		
Misclassified Mamdani:		2	Misclassified Mamdani:		1	Misclassified Mamdani:		5	Misclassified Mamdani:		1
Misclassified Sugeno:		4	Misclassified Sugeno:		1	Misclassified Sugeno:		6	Misclassified Sugeno:		2
Correct classification rate for all the experiments with Mamdani-type FIS:											91%
Correct classification rate for all the experiments MSE with Sugeno-type FIS:											87%

Table 5 also presents the average MSE for every damage category separately for both models. It is obvious that for both models, the average MSE is lower in the 1st damage category, in the same range of values in the 2nd and 3rd category and higher in the 4th damage category. This was expected since, according to Table 1, the MISDR value range is narrow for the category 1, in the same range of categories 2 and 3, and very wide for category 4. Indeed, for the 4th damage category, there is no upper limit. In order to estimate accurately the MISDR value for seismic signals that belong in this category, like in case of the seismic event No.1 (Kobe), more seismic signals of that intensity are required. The FIS in neither model can predict accurately this value since the training test does not comprise seismic events of that range of MISDR values.

The ability of the two models to classify the damage into damage categories is also examined, according to the estimated MISDR values. In Table 4 the misclassified seismic signals are marked in bold. Correct classification rates of 91% are achieved with the Mamdani-type FIS, while 87% with the Sugeno-type FIS.

In a second experimental approach, the training process exploits eighty signals and the testing process twenty signals, randomly selected every time. The experiment takes place one hundred times for statistical reasons in order to achieve convergence. Table 6 summarizes the results, presenting the minimum, maximum and the median values of the MSE utilizing both models. The minimum, maximum and the median values of the MSE are 0.06, 1.15 and 0.21, respectively for the Mamdani-type FIS. The median value arising from the second experimental approach is close to the total average MSE value (0.253) of the first experimental approach. Similarly, the minimum, maximum and the median values of the MSE are 0.08, 1.07 and 0.23, respectively for the Sugeno-type FIS. The median value arising from this approach is close to the total average MSE value (0.289) of the first experimental approach.

This observation justifies the use of the proposed FIS for the MISDR estimation. Based on these findings, one may claim that the Mamdani type FIS outperforms the Sugeno-type FIS in case of the examined structural damage estimation problem.

Table 5. MSE with Mamdani and Sugeno FIS (total average MSE for both models is marked in bold font).

No. of event	MSE		No. of event	MSE		No. of event	MSE		No. of event	MSE	
	Mamdani	Sugeno		Mamdani	Sugeno		Mamdani	Sugeno		Mamdani	Sugeno
1	8.762	8.762	26	0.005	0.176	51	0.504	0.130	76	0.003	0.548
2	0.005	0.563	27	0.012	0.250	52	0.397	0.212	77	0.010	0.011
3	0.303	0.706	28	0.078	0.029	53	0.063	0.109	78	0.006	0.005
4	0.722	0.722	29	0.003	0.005	54	0.740	0.160	79	0.002	0.593
5	0.000	0.000	30	0.002	0.010	55	0.026	0.026	80	0.068	0.122
6	0.476	0.036	31	0.036	0.036	56	0.212	0.023	81	0.003	0.061
7	0.397	0.020	32	0.518	0.410	57	0.144	0.000	82	0.001	0.001
8	0.462	0.008	33	0.012	0.270	58	0.500	0.100	83	0.029	0.029
9	0.384	0.384	34	0.270	0.144	59	0.792	1.103	84	0.017	0.048
10	0.303	0.303	35	0.000	0.000	60	0.116	0.314	85	0.001	0.000
11	0.001	0.980	36	0.048	0.040	61	0.360	0.292	86	0.032	0.058
12	1.392	1.232	37	0.689	0.212	62	0.672	1.145	87	0.040	0.008
13	0.004	0.048	38	0.004	0.012	63	0.068	0.102	88	0.002	0.001
14	0.010	0.010	39	0.023	0.017	64	0.048	0.410	89	0.002	0.034
15	0.084	0.774	40	0.058	0.212	65	0.008	0.008	90	0.012	0.003
16	0.096	0.096	41	0.084	0.078	66	0.008	0.073	91	0.040	0.011
17	0.221	0.102	42	0.084	0.003	67	0.003	0.000	92	0.012	0.033
18	0.185	0.810	43	0.176	0.040	68	0.270	0.624	93	0.012	0.014
19	0.410	0.397	44	0.002	0.000	69	0.020	0.011	94	0.005	0.007
20	0.008	0.250	45	0.023	0.578	70	0.012	0.022	95	0.003	0.003
21	0.689	0.160	46	0.260	0.250	71	0.010	0.017	96	0.000	0.000
22	0.325	0.672	47	0.058	0.656	72	0.010	0.000	97	0.000	0.000
23	1.440	0.410	48	0.221	0.563	73	0.004	0.000	98	0.004	0.001
24	0.014	0.336	49	0.176	0.176	74	0.002	0.002	99	0.005	0.002
25	0.012	0.348	50	0.476	0.144	75	0.001	0.010	100	0.003	0.003
4th damage category		3rd damage category		2nd damage category		1st damage category					
Mean MSE Mamdani:		0.668	Mean MSE Mamdani:		0.133	Mean MSE Mamdani:		0.198	Mean MSE Mamdani:		0.012
Mean MSE Sugeno:		0.725	Mean MSE Sugeno:		0.172	Mean MSE Sugeno:		0.196	Mean MSE Sugeno:		0.064
Average MSE for all the experiments with Mamdani-type FIS:											0.253
Average MSE for all the experiments MSE with Sugeno-type FIS:											0.289

Table 6. Minimum, median and maximum MSE of MISDR estimation for one hundred trials of randomly selected training and testing sets with Mamdani and Sugeno FIS.

	Minimum	Median	Maximum
MSE Mamdani	0.06	0.21	1.15
MSE Sugeno	0.08	0.23	1.07

5. CONCLUSIONS

In this paper, the performance of two types of FIS is examined; a Mamdani-type FIS and a Sugeno-type FIS for structural damage estimation. The Mamdani-type FIS is primarily developed. The FIS is combined with a GA to tune optimally its MFs. In the Sugeno-type FIS, MFs and rule-base are designed to be same as in the Mamdani-type FIS. One hundred natural and artificial earthquake signals are utilized to train and test the proposed models. The FIS models are trained to estimate the MISDR value induced by a seismic signal in a certain structure. Every tested seismic signal is inserted as input to the FIS, in terms of eight selected seismic parameters.

Results reveal that the two models perform similarly in estimating the MISDR value since the average MSE of all experiments is almost the same; 0.253 for Mamdani FIS and 0.289 for Sugeno FIS. When MISDR estimation values are assigned to damage categories, correct classification of up to 91% is achieved with the Mamdani FIS, while 87% with the Sugeno FIS. Thus, for the given problem of MISDR estimation, the Mamdani-type FIS is proven to be a better choice.

6. REFERENCES

- Andreadis I, Tsiftzis Y, Elenas A (2007). Intelligent seismic acceleration signal processing for structural damage classification. *IEEE Transactions on Instrumentation & Measurement*, 56(5):1555–1564.
- EC2 (2000). Eurocode 2: Design of Concrete Structures - Part 1: General Rules and Rules for Buildings, *European Committee for Standardization*, Brussels, Belgium.
- EC8 (2004). Eurocode 8: Design of Structures for Earthquake Resistance - Part 1: General Rules, Seismic Actions, and Rules for Buildings, *European Committee for Standardization*, Brussels, Belgium.
- Elenas A, Meskouris K (2001). Correlation study between seismic acceleration parameters and damage indices of structures. *Engineering Structures*, 23(6): 698–704.
- Gao JS, Xu XH, He C (2012). A study on the control methods based on 3-DOF helicopter model. *Journal of Computers*, 7: 2526–2533.
- Huang NE, Shen Z, Long SR (1998). The empirical mode decomposition and the Hilbert spectrum for nonlinear and non-stationary time series analysis, *Proceedings of the Royal Society A*, 454: 903–995.
- Kappos AJ (1990). Sensitivity of calculated inelastic seismic response to input motion characteristics, *Proceedings of the 4th U.S. National Conference on Earthquake Engineering*, 25–34.
- Kaya M, Alhaji R (2011). Genetic algorithms based optimization of membership functions for fuzzy weighted association rules mining, *Proceedings of Symposium on Computers and Communications ISCC*, 110–115.
- Mamdani EH (1977). Applications of fuzzy logic to approximate reasoning using linguistic synthesis. *IEEE Transactions on Computers*, 26(12): 1182–1191.
- PEER Ground Motion Database (2017). Pacific Earthquake Engineering Research Center, [Online]. Available: <http://ngawest2.berkeley.edu/>
- Reinhorn AM, Roh H, Sivaselvan M, Kunnath SK (2009). IDARC 2D Version 7.0: A Program for Inelastic Damage Analysis of Structures, *MCEER Technical Report- MCEER-09-0006*, State University of New York, Buffalo.
- Sivanandam SN, Deepa S N (2008). Introduction to Genetic Algorithms, Springer Verlag, Germany.
- Song ZY, Song XL, Liu CY, Zhao YB (2013). Research on real-time simulation and control of linear 1-stage inverted pendulum. *Journal of Computers*, 8: 896–903.
- Structural Engineers Association of California (SEAOC) (1995). Vision 2000: Performance based seismic engineering of buildings, Sacramento, California.
- Sugeno M (1977). Fuzzy measures and fuzzy integrals: a survey in fuzzy automata and decision processes, Gupta MM et al. eds., New York: North Holland.
- Tang KS, Man KF, Liu ZF, Kwong S (1998). Minimal fuzzy memberships and rules using hierarchical genetic algorithms. *IEEE Transactions on Industrial Electronics*, 45(1): 162–169.

- Tsiftzis I, Andreadis I, Elenas A (2006). A Fuzzy system for seismic signal processing, *Proceedings of the IEE Vision, Image & Signal Processing*, 153(2): 109–114.
- Vrochidou E, Alvanitopoulos P, Andreadis I, Elenas A, Mallousi K (2014). Synthesis of artificial spectrum-compatible seismic accelerograms. *Institute of Physics, Journal of Measurement Science & Technology*, 25(8): 1–14.
- Vrochidou E, Alvanitopoulos P, Andreadis I, Elenas A (2016). Structural Damage Estimation in Reinforced Concrete Mid-Rise Structure Based on Time Frequency Analysis of Seismic Accelerograms. *IET Science, Measurement & Technology*, 10(8): 900–909.
- Wu Z, Huang NE (2009). Ensemble empirical mode decomposition: a noise-assisted data analysis method. *Advances in Adaptive Data Analysis*, 1: 1–14.
- Zadeh LA (1965). Fuzzy sets. *Information and Control*, 8(3): 338–353.
- Zhao GY, Shen Y, Wang YL (2013). Fuzzy PID position control approach in computer numerical control machine tool. *Journal of Computers*, 8: 622–629.